ROBOTIC REMOVAL OF EV-LIB-PACK LIDS

Abu Islam[1], Matthew DeHaven[1], Nenad Nenadic[1]
[1]Rochester Institute of Technology, 1 Lomb Memorial Dr, Rochester, NY 14623

Primary Topic Area: Innovative Remanufacturing Technologies
Secondary Topic Area: Building a Sustainable Circular Economy for Materials & Products

Abstract

With the growing market penetration of electric vehicles (EVs), their end-of-life (EOL) considerations require careful attention. Chief among them is the lithium-ion battery (LIB) pack disassembly, which requires a high degree of automation to accommodate increasing volumes. However, robotic solutions for EV LIB disassembly must be sufficiently flexible to handle diverse pack designs. We describe the design, development, and testing of two end effectors, one for fastener removal and the other for lid removal, using four distinct pack enclosures of different designs. The solution for the autonomous detection and loosening of fasteners employed commercial 2D and 3D cameras mounted on the wrist of a robotic arm. The solution for the fastener removal had three key processing steps: 1) approximate localization of fasteners on the lid using images from a 2D camera, 2) precise localization and orientation based on a 3D camera, and 3) loosening of fasteners using a drive. Tests on multiple LIB pack enclosures of different shapes and sizes, placed in several orientations relative to the robotic arm, showed that the success rate of the proposed solution exceeded 90%, on average. The effectiveness of the solution for different pack designs and orientations demonstrated the autonomy and generality of the approach. Once effectiveness was established, the solution was improved to increase efficiency. We describe the iterative improvements that reduced the initial fastener detection and loosening process from approximately 20 seconds per fastener to ≈10 seconds per fastener. Because the selected hardware limited additional time reduction, a discussion on the potential for further acceleration, based on alternative image-capturing hardware, was included. In addition, the end effector contained a magnetic pick-off for removing the loosened fasteners and dropping them into a bin. This process was considered separately because a human typically employs his second hand for collecting fasteners. To attain a comparable end-to-end speed, a separate robotic arm should be considered for fair comparisons. The end effector for lid removal employed springs to conform to the height variation of some LIB pack designs. The paper includes illustrative frames of key operations of the effectors and the tool for exchanging between the two end effectors.

Introduction and Motivation

As detailed in the authors previous paper[1] according to market analysis-the number of electric vehicles (EVs) produced annually will increase more than eight-fold, from 3.1millon in 2020 to 26.9 million by 2030 [2]. The International Energy Agency (IEA) expects even higher growth, predicting that 51% of all new vehicles produced in 2030 will be electric. The EV batteries reach their end of life (EOL) when the capacity fades to 70-80% of new. The used batteries have a potential for secondary uses in less-demanding applications, such as grid storage, where batteries perform multiple functions, including peak shaving and firming of the renewables [3]. Introducing automation to the disassembly process and accelerating the condition assessment of used modules will facilitate the repurposing of EV batteries after their primary EOL in less demanding applications with increased throughput, yield, and safety for the remanufacturers. However, there are several challenges associated with such automation. The EV LIB pack design has yet to be standardized, as illustrated in Figure 1, which shows four different packs of different sizes and form factors used in the study. The diversity of designs, modules' topologies, spatial arrangements of modules, and cell chemistries make EV LIB reuse very challenging. Even the batteries of the same model could have differences in the enclosure from batch to batch. That necessitates an intelligent disassembly process, where instead of performing all the tasks using deterministic programming routines, there is a need to make instantaneous decisions based on the situation at hand.

Figure 1: Four different battery packs used in the study.

The previous work by the authors elaborated the state of the art, technology approach of using computer vision and end effector design for fastener removal and presented the preliminary results. This paper provides the current status of the work by describing the steps taken in increasing the productivity of fastener removal and extending the technology to angled fasteners. It also describes the end effector design for lid removal and describes the preliminary results. It will summarize the author's evaluation of feasibility of cutting off the lid and draw conclusions.

Review of Related Work

Much of the state of the art presented in the previous work suggested that lack of standardization of the battery manufacturing process and safety issues are the main challenges for automating the disassembly of LIB packs. The predominant direction of existing research is to adopt a semiautomatic disassembling process with humans in the loop and robots working collaboratively with humans.

More recently, Kaarlela et al. [4] provides a overview of current state of art in robotic disassembly and outlines future directions. It reiterates the need for human robot collaboration, AI and challenges due to lack of standardized designs of battery packs. Rasterarpannah[5] et.al. describes a surface exploration method to detect hexagonal fasteners and demonstrates ~50 sec time required to remove a fastener. Qu et al. [7] conducted an empirical study on disassembling packs… the speed of removing fasteners was approximately 20 seconds per fastener. Rastegarpanah et.al [6] describes a semi-autonomous system with mixed reality for EV pack disassembly resulting in a semiautomatic fastener removal time of ~6 sec(Need to st udy more).

Rettenmeier et al. [8], has conducted perhaps the most comprehensive analysis of cutting off the top cover. In that work the authors concur that individual fastener removal may be cumbersome due to the sheer variety of fasteners that may be out there and issues with their detectability and accessibility etc. They conclude that cutting off the top cover may be advantageous if the cutting mechanism does not touch or interfere with the battery pack contents such as busbars, modules, BMS etc. They evaluated, compared and contrasted several technologies. They favored laser or plasma based cutting technologies due to their non-contact, fast, flexibility and scalability, but expressed concerns in managing heat and splatters that can potentially damage critical internal components. They eliminated the use of water jet cutting due to the risk of seeping water and contaminants inside the pack with high voltage components. They do mention the use of Shear or Cutting knife which could minimize some of the problems of laser cutting but could be very slow and difficult to keep the cutter from inside the pack. Ultrasonic cutting is mentioned as a possibility since no liquid is needed, but very limited information exists on its effect on internal components if leaked and how effective it could be in cutting different kinds of metals. However, the paper does not discuss any implementation experiences with any of the technologies. Trumpf [9] Laser Company advertises several trade magazines, the availability of a laser system to automatically cutoff and remove EV pack cover. But no information could be found on anyone implementing the system.

Technology Approach

The technology approaches for fastener and lid removal is described in the following sections.

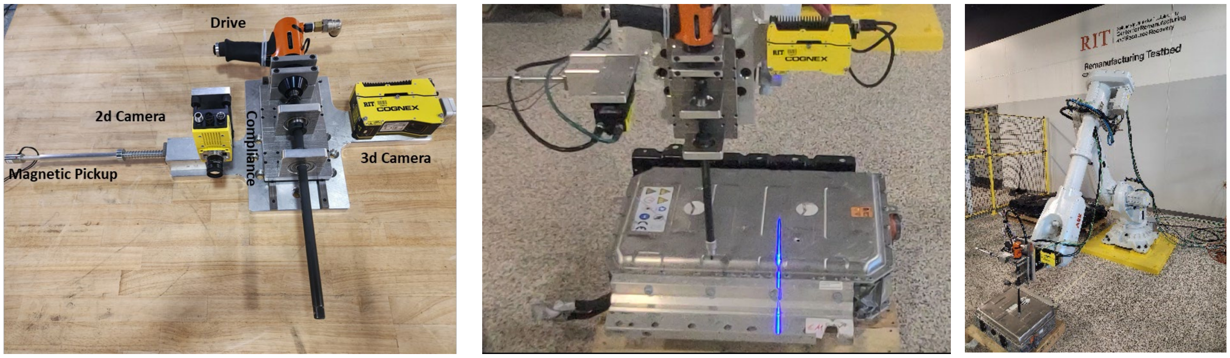

(a) (b) (c)

Figure 2: (a) Fastener removal End effector details (b) End effector mounted (c) Disassembly robotic cell.

Fastener removal

The fundamental approach taken for the fastener removal is to use vision systems to detect the Battery pack, detect the locations and types of the fasteners and them use the information to guide the robotic arm to pick up the right tools to remove the fasteners. The development of the end effector, vision system selection and the results of bench test was described in the prior work [1]. Here we describe the performance tests of the system end-to-end functionality, approaches to reduce the time of fastener removal, and the process of transforming object-orientation information from the representation of the 3D camera to that of the robotic arm. Further improvements to the end effector were made by mounting the 2D camera on the wrist of the robotic arm in addition to the 3D camera instead of the overhead gantry as shown in Figure 2(a). This enabled automatic vertical height adjustment of the camera to use its full field of view irrespective of the size of the pack. The end effector mounted to the robot is shown in Figure2(a) and the robotic cell in Figure 2(c). Fastener removal steps are detailed in Figure 3. The 2D camera identified approximate locations of the fasteners within +/- 5mm, 3D camera used that information to scan the fasteners and accurately determine their precise (within +/- 0.5mm) location and orientation. We found that this was not enough to ensure engagement of the tool with the fastener. A custom tool (Smaller size for Torx, Larger size for Hex) with more clearance needed to be used to provide more lateral compliance. In addition, the tool needed to be oscillated with circular motion to ensure proper engagement.

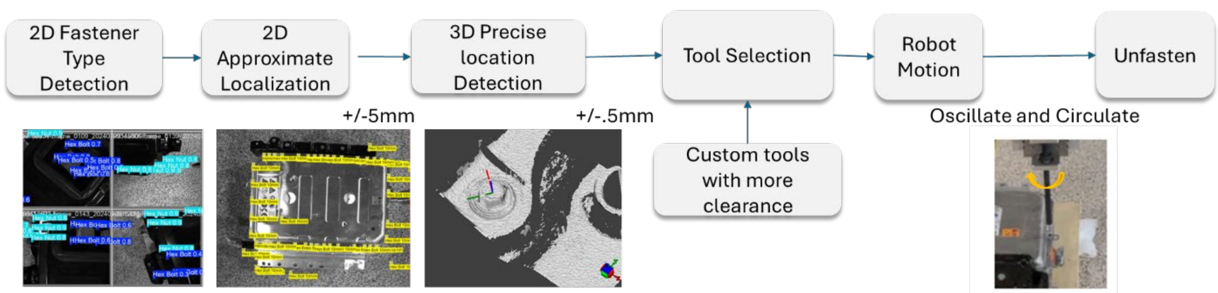

Figure 3: Fastener Removal Sequence

Performance testing

Tests for quantifying the performance of the top cover fastener removal process consisted of placing different packs under different orientations, using 2D and 3D cameras for fastener detection, and measuring the success rate of the end-to-end process. The robot operated on each pack five times, ones for each pack placement. (including 180 rotations in the plane and a few smaller random rotations) before performing end-to-end fastener removal tests consisting of 2D detection, 3D localization, and extraction. The number of fasteners removed measured the success. Table 1 shows the result for the first of three packs. The cumulative success rate was 99.5%. The overall time for fastener removal was 14 minutes and 34 seconds, or 21.1 seconds per fastener.

Table 1: Success rate on fastener removal on a small pack with torx fasteners

Test image	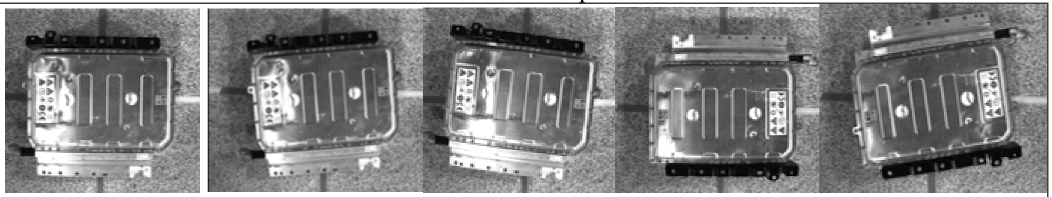				
Fasteners removed	40/40	40/40	40/40	39/40	40/40
Success rate [%]	100	100	100	97.5	100

Table 2 shows the result for the second pack. The cumulative success rate was 93%. The overall time for fastener removal was 12 minutes and 44 seconds, or 20.6 seconds per fastener.

Table 2: Success rate on fastener removal on a large pack with torx fasteners

Test image	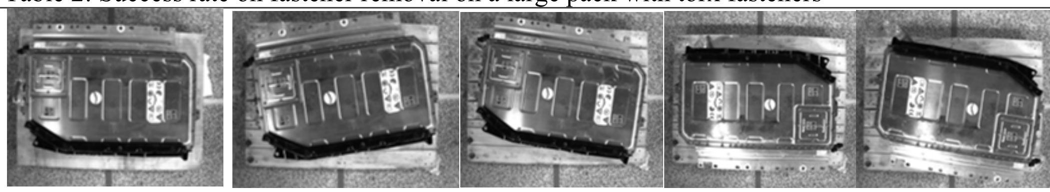				
Fasteners removed	35/37	34/37	32/37	36/37	35/37
Success rate [%]	94.6	91.9	86.5	97.3	94.6

Table 3 shows the result for the third pack. The cumulative success rate was 95.3%. The overall time for fastener removal was 15 minutes and 6 seconds, or 26.6 seconds per fastener.

Table 3: Success rate on fastener removal on a pack with small hex fasteners

Test image	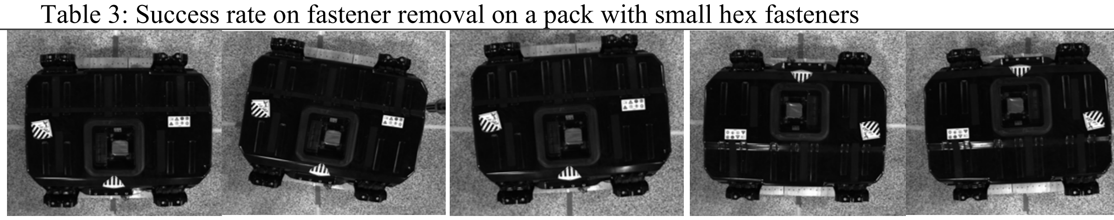				
Fasteners removed	32/34	32/34	32/34	33/34	33/34
Success rate [%]	94.1	94.1	94.1	97.1	97.1

The third pack had a black cover. The 3D camera required that settings be adjusted before the performance shown in Table 3 was attained. The key changes needed to enable detection of fastener on black cover was to increase the 3D scanner exposure time from .3ms to .8 ms and fine tuning the threshold for feature acceptance.

Performance improvements

The reliability of fastener detection, localization, and loosening was encouraging, but the associated time was too long. Note that magnetic removal was excluded from the investigation during this development phase. Table 5 and Figure 3 summarize the results. The reference time for removing a single fastener of 23 seconds was reduced to approximately 10 seconds. In addition, the results were compared to manual fastener removal, which required only 3.8 seconds per fastener. The process cannot be further accelerated with the current 3D camera for accurate fastener localization.

The nomenclatures of rows and columns of Table 5 are described as follows:

Localization step takes snapshots of the battery pack and detects approximate locations of the fastener. These approximate locations are used for path planning to send the end effector near the detected fasteners. The fasteners are then scanned by the 3d laser scanner for exact 3d location of the fasteners that are used to remove fasteners in subsequent operations. Tool *engage* step is the time taken by the tool end to go from is current position to the detected fastener location in the previous step.

In *wobble,* step the tool end is jiggled in X-Y and circular motion to ensure that the tool end engages with the fastener.

In *unscrew***,** as the name suggests this steps simple unbolts the fastener.

Finally in *disengage***,** This step removes the tool end and end effector from the fastener to a clearance distance.

Cycle Time Improvement Methodologies:
In *initial/Baseline* tests*,* times were captured in the base configuration of the developed system, where the fasteners were detected using deep learning capabilities within the Cognex Camera and approached in the order of probabilities of detection. In *ordered Fasteners* tests, the fasteners were arranged in order of proximity to one another to the end effector did not have to spend time going back and forth between fasteners that may be far apart

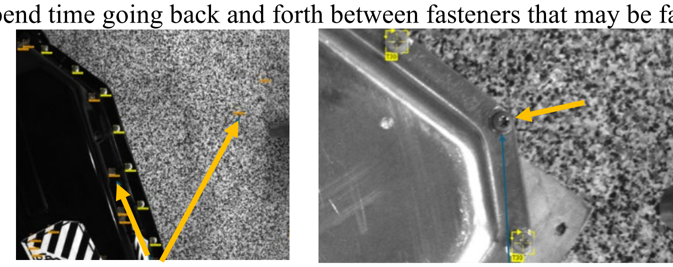

(a) (b)

Figure 4: Examples of detection errors (a) false positives (b) missed detections

In *YOLO(2D)* method, instead of processing the images in Cognex Camera on board processor, the 2D images were exported using FTP protocol to the control PC, where the images were used to train a YOLO model offline and detect the fasteners. In *faster wobble* method, the wobble was executed at a faster speed from 8mm/s to 30mm/s
In *faster scan and motion***,** In this step the scanning and end effector speed of motion was increased from 20mm/s to 50mm/s. In *single scan and lower Z*, In this method, instead of scanning fasteners one at a time, all the fasteners in one edge of the battery pack was scanned at once and the Z distance of tool withdrawal was decreased to reduce travel time.

Table 4: Progressive improvements in reduction of time in seconds, per fastener.

	Localization	Tool Engage	Wobble	Unscrew	Disengage	Total
Initial	9	4	4.0	4.0	2	23.0
Ordered fasteners	6	3	3.0	3.0	3	18.0
YOLO (2D)	6	4	3.0	3.0	1	17.0
Faster wobble	6	4	1.7	3.0	1	15.7
Faster scan & motion	3	2	2.0	3.0	2	12.0
Single scan & lower z	3	1	2.0	3.0	1	10.0
Manual	0	1	0.0	1.8	1	3.8

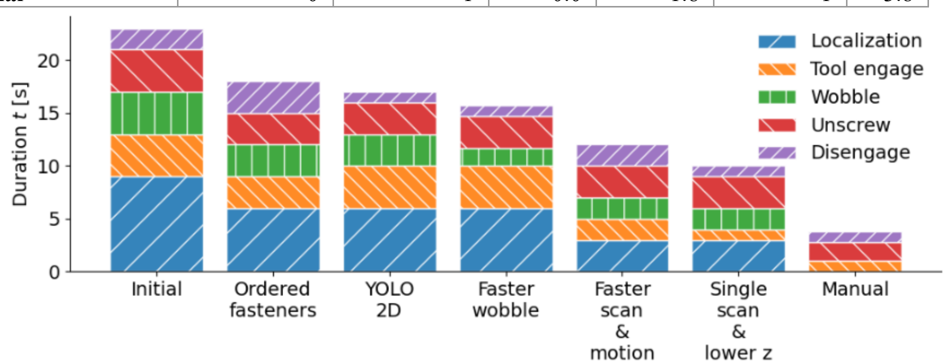

Figure 5: Progressive improvements in reducing fastener extraction time.

Since its introduction [10], the You Only Look Once (YOLO) object detection and classification algorithm has been embraced by the CV/ML community and continuously improved (see, e.g., [11]).
Additional improvements could be attained with different hardware, with different underlying physical principles, for accurate 3D localization and orientation detection. The Discussion section provides more details on the advantages of alternative hardware selection.

Tilted fasteners

In the majority of battery packs, all fasteners were perpendicular to the lid surface, and the time study was concerned only with only those types. However, a subset of LID packs contained tilted fasteners, as shown in Figure 5a. To remove them, the 3D scanner must measure the angle of the fastener so that the robot can be properly aligned, but the

Cognex vision software and the ABB robot employ different object-orientation representations. The output of the Cognex scanner must be converted as follows. The camera's representation is given by two scalars tilt θ and tilt direction ϕ, as shown in Figure 5b.

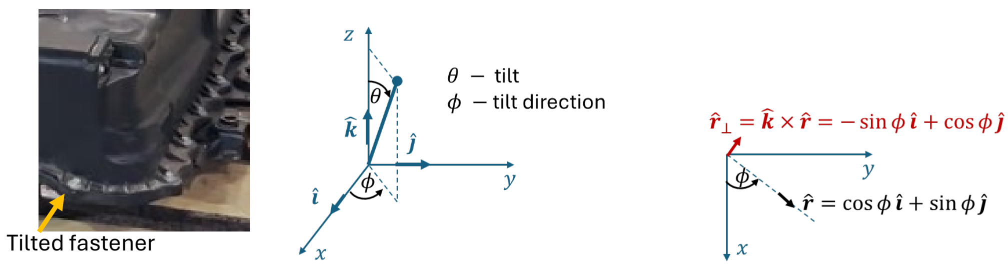

(a) (b) (c)

Figure 6: (a) pack enclosure with tilted fasteners (b) Cognex representation of a fastener (c) top view showing the unit vectors in the direction of the tilt and its normal.

ABB specifies orientation of an object with a quaternion $\boldsymbol{q}$. Mathematical form of $\boldsymbol{q}$ is, e.g., (see [12])

$$\boldsymbol{q} = \left(\cos\frac{\theta}{2}, \hat{\boldsymbol{n}}\sin\frac{\theta}{2}\right), \tag{1}$$

where θ is the tilt angle and $\hat{\boldsymbol{n}}$ is the unit vector in the direction of the axis about which the rotation takes place. In the xy-plane (see Figure 5b) we readily identify the unit vector along ϕ, denoted by $\hat{\boldsymbol{r}}$. The desired unit vector must be perpendicular to $\hat{\boldsymbol{r}}$, i.e., $\hat{\boldsymbol{n}} = \hat{\boldsymbol{r}}_\perp = -\sin\phi\,\hat{\boldsymbol{\imath}} + \cos\phi\,\hat{\boldsymbol{j}}$ (see Figure 5c), which when plugged into Eq. (1) yields a quaternion representation

$$\boldsymbol{q} = \left(\cos\frac{\theta}{2},\ -\sin\phi\sin\frac{\theta}{2}, \cos\phi\sin\frac{\theta}{2}, 0\right) \tag{2}$$

The reference position of the ABB local coordinate system of the end effector points down $\boldsymbol{q}_{\mathrm{ref}} = (0,0,-1,0)$, we need to transform the quaternion representation into the ABB's coordinate system by multiplying quaternions

$$\boldsymbol{q}\boldsymbol{q}_{\mathrm{ref}} = \left(\cos\phi\sin\frac{\theta}{2}, 0, -\cos\frac{\theta}{2}, \sin\phi\sin\frac{\theta}{2}\right) \tag{3}$$

Finally, to adhere to ABB's convention of positive first component q_0, we negate the quaternion when $q_0 < 0$.

$$\boldsymbol{q}\boldsymbol{q}_{\mathrm{ref}} = \begin{cases} \left(\cos\phi\sin\frac{\theta}{2}, 0, -\cos\frac{\theta}{2}, \sin\phi\sin\frac{\theta}{2}\right), & \cos\phi\sin\frac{\theta}{2} \geq 0 \\ \left(-\cos\phi\sin\frac{\theta}{2}, 0, \cos\frac{\theta}{2}, -\sin\phi\sin\frac{\theta}{2}\right), & \cos\phi\sin\frac{\theta}{2} < 0 \end{cases} \tag{4}$$

The solution was implemented in Python and tested on a LIB pack enclosure with tilted fasteners. Figure 6 shows frames from a video capturing the demonstration of localization and detection of a tilted fastener, followed by the successful removal. Figure 6a shows the initial laser scan (the purple line), with the end effector approximately perpendicular to the lid surface. Figure 6b shows the next step where the end effector tilted by angle θ and approached the fastener, and Figure 6c shows the end effector engaging with the fastener.

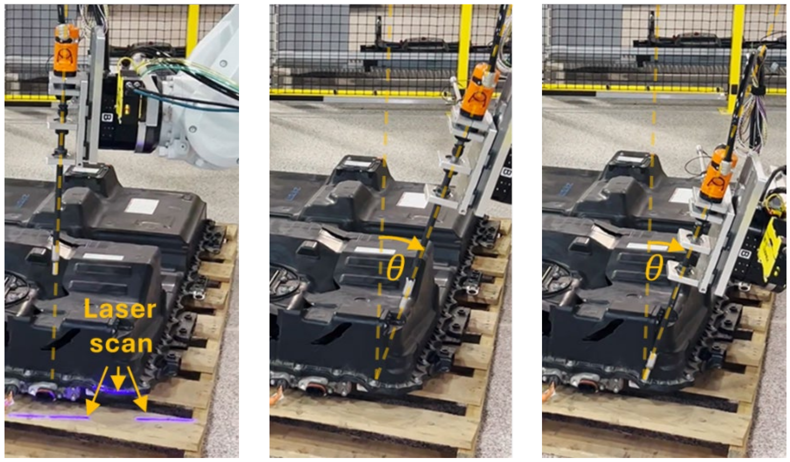

(a) (b) (c)

Figure 7 Removal of a tilted fastener (a) laser-scanning (c) tool tilt and approach (d) fastener engaged

Lid removal

We designed, developed, and built a suction cup gripper for top cover removal (Figure 7). The system features suction cups each capable of lifting approximately 15 pounds, providing a total lift capability of around 60 pounds. The suction cups were mounted on slides to accommodate different battery pack sizes. To handle variations in top cover depths and sections, each suction cup was equipped with spring mounting for compliance.

(a) (b)

Figure 8: Suction gripper system (a) CAD design (b) built gripper.

Figure 8 shows images of lid-removal demonstrations for different packs. Two packs had flat, solid lid, and one had uneven, slightly flexible lid. Note that the compliance lengths were different in Figure 8c, adapting to the heights of different parts of the lid.

(a) (b) (c)

Figure 9: Lid-removal demonstration (a) top view of a removal of a rigid flat lid (b) side-view removal of a rigid flat lid (c) side-view removal of an uneven, slightly flexible lid.

The robotic arm was equipped with a tool exchanger to enable smooth automatic. We designed and built the tool changer bracket that enables installation of the tool changers to the robot and the tools for rapidly changing from fastener removal to lid removal end effectors, as shown in Figure 9. The two cameras were installed on the fixed side of the tool exchanger and can be used to support CV associated with both fastener removal and lid removal.

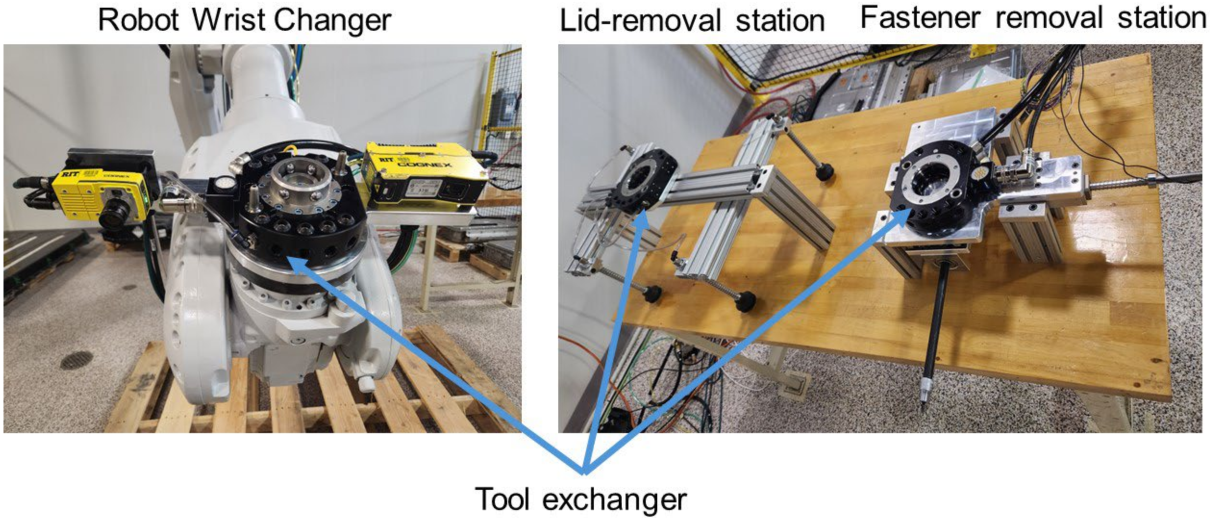

Figure 10: tool exchanger and brackets on the bench top

Discussion

In the prior work, we discussed advantages of alternatives to commercial 2D and 3D imaging equipment, and built-in CV/ML solutions [1]. We claimed that replacing commercial CV/ML solutions and on-board computing within smart industrial cameras with custom CV/ML solutions based on open-source software and the central computer has the potential for accelerated development and superior results. Using structured light instead of laser scanning holds the potential to further improve the performance. Three key advantages of structured-light over laser-scanning solutions are speed, flexibility, and accuracy. The structured-light camera (e.g. Zivid) generates point clouds in under one second, compared to Cognex's eight-second acquisition and processing cycle. Additionally, the structured-light camera outputs standard-format point clouds compatible with open-source libraries, while Cognex employs proprietary algorithms with complex parameterization. Laser line scanners require synchronized motion with the workpiece for image generation. When mounted on a robot wrist, inherent controller delays create ±20 ms timing errors between scan initiation and robot movement, producing >1 mm directional errors. Structured light cameras eliminate this error source through stationary operation. The Zivid camera includes dowel pin holes for precise robot coordinate system alignment.

In addition to fastener removal, we investigated the feasibility of laser cutting and alternative mechanical cutting. The investigation employed the research of literature and analyses of the geometry of the four LIB pack enclosures. The literature identifies challenges with mechanical cutting, including: managing heat and splatters that can potentially damage critical internal components associated with laser cutting; water sipping and causing shorts, associated with water jets; and slow cutting times associated with shear or cutting knife.

Table 5: Comparison of different cutting methods

Operation	Speed	Safety	Messiness	Pick up time
Unscrewing	Slow ~10s/fastener	Best	Best	Significant
Laser Cutting	Fastest: ~5 s/fastener	Laser safety is an issue	Moderate	Not needed
Milling	Moderate: ~5-10 s/fastener	Risk of chips going inside the pack	Worst	Not needed

RIT conducted a study of the laser-cutting requisite path planning accuracy and found that the path tolerances for laser cutting are very tight ($\approx \pm$2-3 mm), which is borderline accuracy for 2D vision. The tolerance for laser cutting (see Figure 9) is very tight $\pm$2 mm, and not attainable with the current path planning accuracy based on the 2D imaging. It is also conceivable that attaching a milling tool to the robot may be appropriate for cutting off the fastener's heads. Table 6 compares the advantages and disadvantages of different cutting methods.

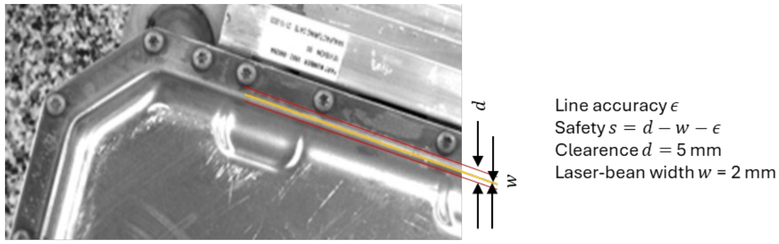

Figure 11: Tolerance for laser cutting

It is the opinion of the authors that despite the technological advances it will not be possible to reduce the time required for automated disassembly to manual disassembly. Industrial robots and cobots are intended for deterministically programmed repetitive tasks, where every task follows a predetermined path to a precise location doing a specific action. Disassembly requires perception of the task (i.e. fastener removal) by tactile and/or vision and make instantaneous decision on how to engage, that requires time. Human beings are adept in perceiving the local situation and reacting without even thinking. When we use a screwdriver to remove a screw, we subconsciously adjust the angle of the driver until we feel the engagement, accomplishing that by programming a robot is non-trivial. It is conceivable to implement a vision and force sensor based closed loop control for automation that that further adds to complexity, maybe time and risks instability.

Conclusion & Recommendations

The study encompassed three primary areas: performance testing of fastener removal, removal of tilted fasteners, and lid removal with end effector exchanger. In addition, it includes a discussion on the potential for lid removal using laser or mechanical cutting.

The test of the effectiveness and reliability of fastener detection, localization, and unthreading, based 2D and 3D cameras, employed three battery enclosures (two metallic reflective, one metallic dark) in multiple orientations. The cumulative rates achieved > 93% success rate. Two enclosures were of metallic reflective types and one was metallic dark, which required modification in the 3D camera parametrization. Process optimization reduced fastener handling time from 20 s to 10 s, approaching the current camera system's limits. Alternative structured-light imaging solutions, such as Zivid cameras, showed potential for further cycle time reduction.

To enable tilted fastener removal, the system transformed the 3D camera's representation of tilt orientation data (angle and direction) into quaternion format suitable to the ABB robot, and then applied quaternion multiplication with the end effector's orientation quaternion to determine the final tool pose.

The custom-designed lid removal end effector employed adjustable spring mechanisms to accommodate varying lid geometries. Testing demonstrated successful removal of both flat lids and those with height variations, with the spring system providing consistent pressure distribution across different surface profiles.

Future work will investigate structured-light camera process improvements and expand capabilities to include module handling and palletization.

Acknowledgments

This material is based upon work supported by the U.S. Department of Energy's Office of Energy Efficiency and Renewable Energy (EERE) under the Advanced Manufacturing Office Award Number DE-EE0007897 awarded to the REMADE Institute, a division of Sustainable Manufacturing Innovation Alliance Corp. In addition, RIT received funding, in part, from New York State Empire State Development under Grant #AC118 that supported the work on this project.

The views expressed herein do not necessarily represent the views of the U.S. Department of Energy or the United States Government or New York State.

References

[1] Islam, A., DeHaven, M., Neipert, M., and Nenadic, N., "Automation for Electric Vehicle Battery Pack Disassembly," *2024 REMADE Circular Economy Technology Summit & Conference*, Washington, DC.

[2] Jones, C., 2021, "Global Electric Vehicle Sales up 39% in 2020 as Overall Car Market Collapses," Businesswire. [Online]. Available: https://www.businesswire.com/news/home/20210208005423/en/Canalys-Global-Electric-Vehicle-Sales-up-39-in-2020-as-Overall-Car-Market-Collapses (July 12, 2021).

[3] Valant, C., Gaustad, G., and Nenadic, N., 2019, "Characterizing Large-Scale, Electric-Vehicle Lithium Ion

Transportation Batteries for Secondary Uses in Grid Applications," Batteries, **5**(1). https://doi.org/10.3390/batteries5010008.

[4] Kaarlela, T., Villagrossi, E., Rastegarpanah, A., San-Miguel-Tello, A., and Pitkäaho, T., 2024, "Robotised Disassembly of Electric Vehicle Batteries: A Systematic Literature Review," J. Manuf. Syst., **74**(February), pp. 901–921. https://doi.org/10.1016/j.jmsy.2024.05.013.

[5] Rastegarpanah, A., Ner, R., Stolkin, R., and Marturi, N., 2021, "Nut Unfastening by Robotic Surface Exploration," Robotics, **10**(3), pp. 1–17. https://doi.org/10.3390/robotics10030107.

[6] Rastegarpanah, A., Contreras, C. A., and Stolkin, R., 2024, "Semi-Autonomous Robotic Disassembly Enhanced by Mixed Reality," ACM Int. Conf. Proceeding Ser., pp. 7–13. https://doi.org/10.1145/3674746.3674748.

[7] Qu, M., Pham, D. T., Altumi, F., Gbadebo, A., Hartono, N., Jiang, K., Kerin, M., Lan, F., Micheli, M., Xu, S., and Wang, Y., 2024, "Robotic Disassembly Platform for Disassembly of a Plug-In Hybrid Electric Vehicle Battery: A Case Study," Autom. 2024, Vol. 5, Pages 50-67, **5**(2), pp. 50–67. https://doi.org/10.3390/AUTOMATION5020005.

[8] Rettenmeier, M., Sauer, A., and Möller, M., 2024, "Laser-Based Battery Pack Disassembly: A Compact Benchmark Analysis for Separation Technologies," Procedia CIRP, **122**, pp. 181–186. https://doi.org/10.1016/j.procir.2024.02.007.

[9] Weber, A., 2024, "New Laser Process Improves EV Battery Recycling," Assembly. [Online]. Available: https://www.assemblymag.com/articles/98589-new-laser-process-improves-ev-battery-recycling.

[10] Redmon, J., Divvala, S., Girshick, R., and Farhadi, A., 2016, "You Only Look Once: Unified, Real-Time Object Detection," Proc. IEEE Comput. Soc. Conf. Comput. Vis. Pattern Recognit., **2016-Decem**, pp. 779–788. https://doi.org/10.1109/CVPR.2016.91.

[11] Wang, C. Y., Bochkovskiy, A., and Liao, H. Y. M., 2020, "Scaled-YOLOv4: Scaling Cross Stage Partial Network," Proc. IEEE Comput. Soc. Conf. Comput. Vis. Pattern Recognit., pp. 13024–13033. https://doi.org/10.48550/arxiv.2011.08036.

[12] Kuipers, J. B., 1999, *Quaternions and Rotation Sequences: A Primer with Applications to Orbits, Aerospace, and Virtual Reality.*, Princeton University Press.

About the Authors

Abu Islam a Research Associate Professor at RIT. received his Ph.D. in Mechanical Engineering from Rensselaer Polytechnic Institute in 1995. His research interests include the use of computer vision, data analytics and artificial intelligence in remanufacturing and health monitoring of machines. He holds a Black Belt in Design for Lean Six Sigma and 26 US Patents.

Matthew Dehaven is a Senior Robotics Engineer at RIT. He received a BS in Mechanical Engineering from RIT in 2004 and a MS in Mechanical Engineering from Florida A&M University in 2008. His research interests include robotics, computer vision, machine learning, and artificial intelligence.

Nenad Nenadic is a Research Associate Professor at RIT. He received Ph.D in Electrical and Computer Engineering from the University of Rochester in 2001. His research interests include sensors, battery systems, automation, and machine learning.